

¹³C Carbonyl Chemical Shielding Tensors: Comparing SCF, MBPT(2), and DFT Predictions to Experiment

NICK GONZALES, JACK SIMONS

Department of Chemistry, University of Utah, Salt Lake City, Utah 84112

Received 20 September 1996; revised 3 December 1996; accepted 4 December 1996

ABSTRACT: In this work, we calculate the ¹³C nuclear magnetic resonance chemical shielding tensors for 18 carbonyl-containing compounds. The many-body perturbation theory (MBPT), self-consistent field (SCF), and density functional theory (DFT) formalisms were used with gauge including atomic orbitals (GIAO) to calculate the shielding tensors. Our data suggest that shielding tensors can be efficiently estimated by performing one MBPT(2) correlated calculation (e.g., at a reference geometry) and SCF-level calculations at other geometries and taking the SCF-to-correlated tensor element differences to be geometry independent. That is, the correlation contribution to the chemical shielding seems to be relatively constant over a considerable range of distortions. Treatment of correlation using DFT methods is shown to not be as systematically reliable as with MBPT(2). Data on 18 carbonyl compounds show that the single largest influence on the shielding tensor is the presence of nearby electron-withdrawing or electron-donating groups. Finally, although good agreement with powder or single-crystal experimental data is achieved for two of three tensor eigenvalues, systematic differences remain for one element; the origins of these differences are discussed. © 1997 John Wiley & Sons, Inc.
Int J Quant Chem 63: 875–894, 1997

Introduction

The advent of modern high-field multipulse nuclear magnetic resonance (NMR) spectroscopy as an analytical tool has given scientists a

valuable noninvasive probe of molecular structure and dynamic behavior. In chemistry, for example, splitting patterns and chemical shifts provide a wealth of knowledge about molecular topology. The nuclear magnetic shielding tensor is so sensitive to the electronic environment that often sites which cannot be distinguished from each other by any other measurement can be distinguished by the differences in their NMR shielding.

However, there remain problems with the quantitative interpretation of the relationship be-

Correspondence to: J. Simons.

Contract grant sponsor: Office of Naval Research.

Contract grant sponsor: National Science Foundation.

Contract grant number: CHE91-16286.

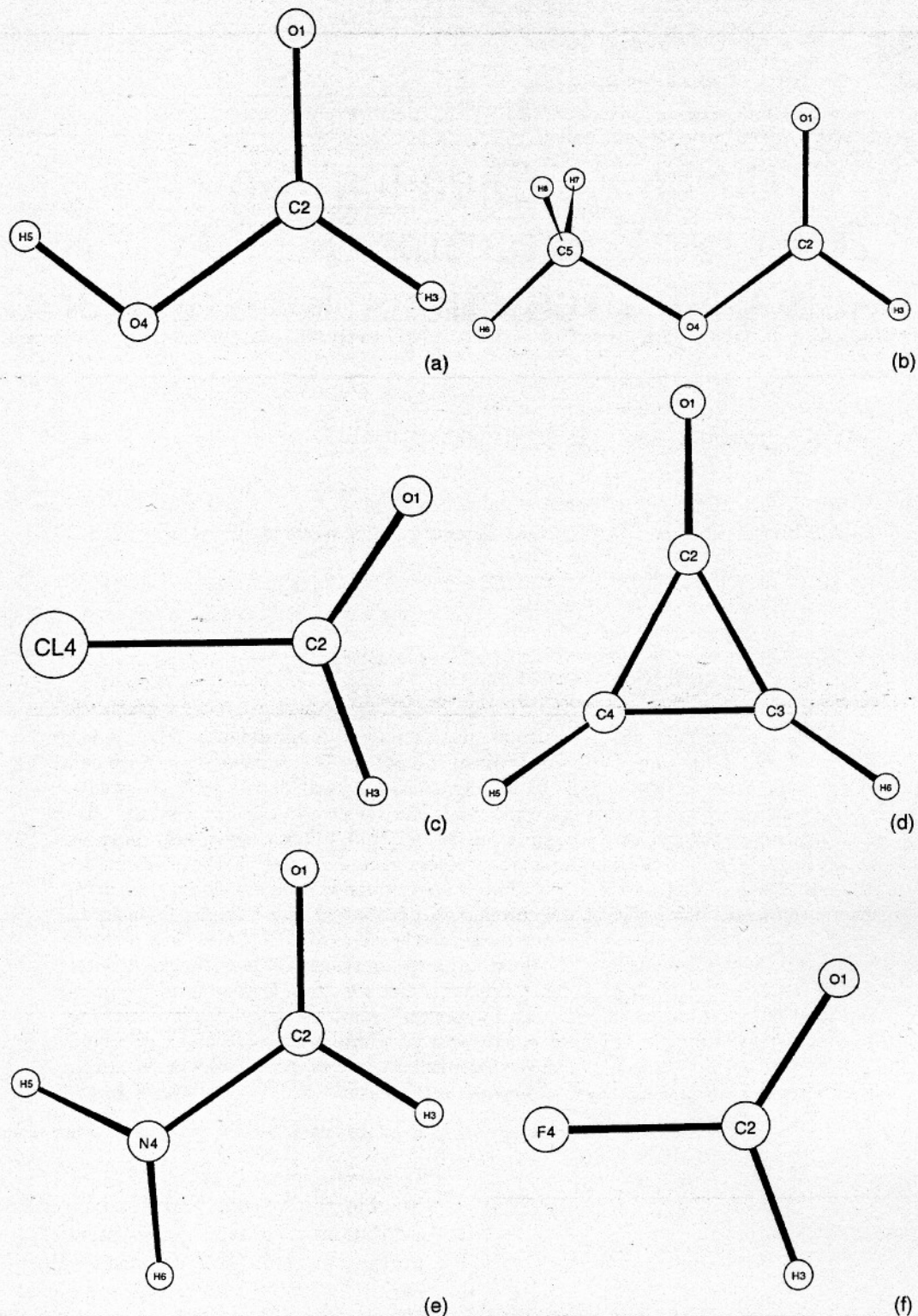


FIGURE 1. Equilibrium geometries for 18 carbonyl-containing compounds. Geometries were optimized at the MBPT(2)/TZP level. See Table I for point group symmetry, energy, and optimized geometrical parameters. (a) HO-CHO, (b) CH₃O-CHO, (c) Cl-CHO, (d) 2-Cyclopropene-1-one, (e) NH₂-CHO, (f) F-CHO, (g), CH₃COOH, (h) CH₃COOCH₃, (i) Bicyclo[1.1.1]pent-2-one, (j) NC-CHO, (k) NH₂COCH₃, (l) H₂C=CH-CHO, (m) H₂CO, (n) CH₃CHO, (o) Cyclobutanone, (p) Tricyclo[1.1.1.0^{1,3}]pent-2-one, (q) CH₃COCH₃, (r) Cyclopropanone.

tween the second-rank chemical shielding tensor (CST) and molecular structure. Accurate ab initio calculations of shielding tensors have recently become more accessible [1] and are now able to be directly compared to experimentally measured tensors. In the present work, we attempt to contribute to this understanding by addressing the following issues specifically for ¹³C carbonyl

nuclei:

1. How does geometrical distortion such as ring strain or CO bond elongation affect the chemical shielding tensor of a given ¹³C center? In other words, can one expect to use differences in tensor values among a series of compounds as quantitative probes of bond

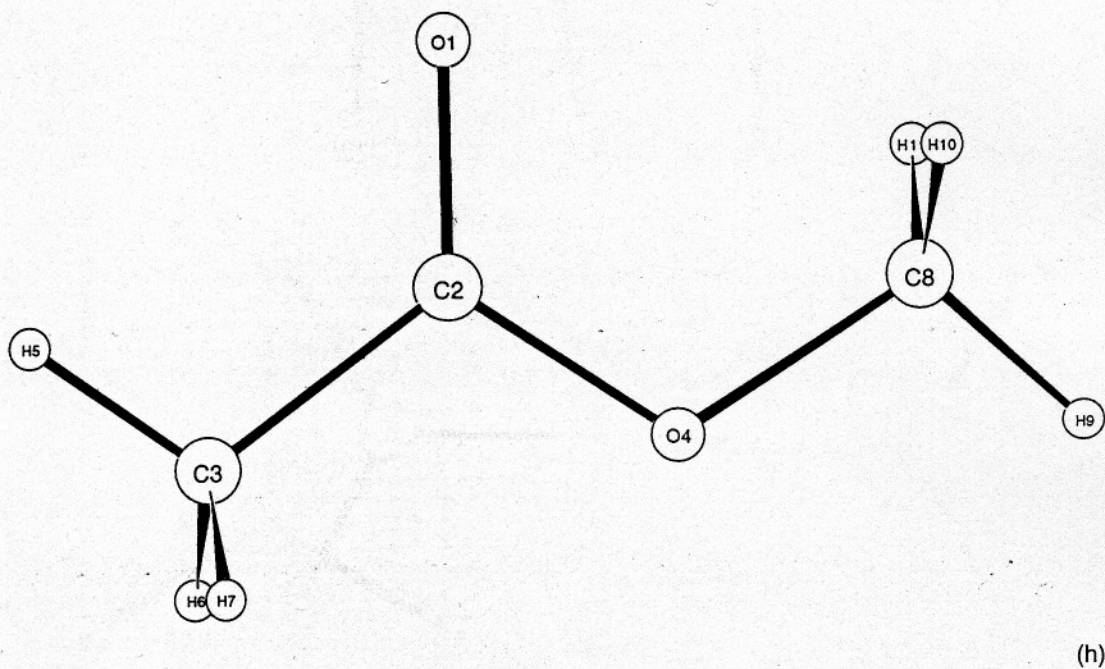
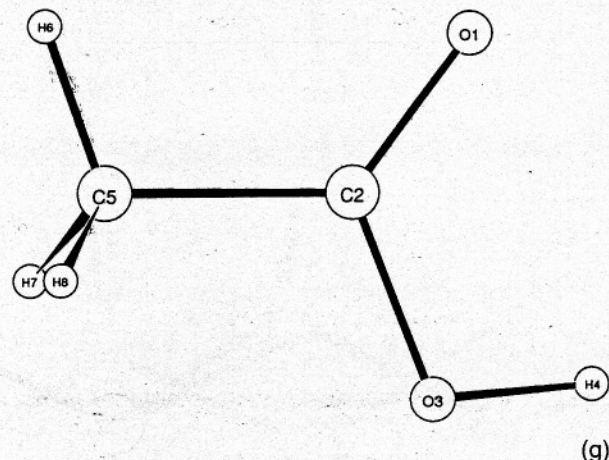


FIGURE 1. (Continued)

lengths, interbond angles, and dihedral angles?

- How quantitatively different are the self-consistent field (SCF), many body perturbation theory [MBPT(2)], and density functional theory (DFT) predictions of chemical shielding tensors? That is, must one use correlated level theory to compute tensors accurate

enough to assist in interpreting experimental data, and if so, is the less CPU-intensive DFT treatment adequate?

- How does the chemical shielding tensor change when different functional groups are added to a molecule in close proximity to the ^{13}C center? Does the introduction of an electron-withdrawing or donating group sys-

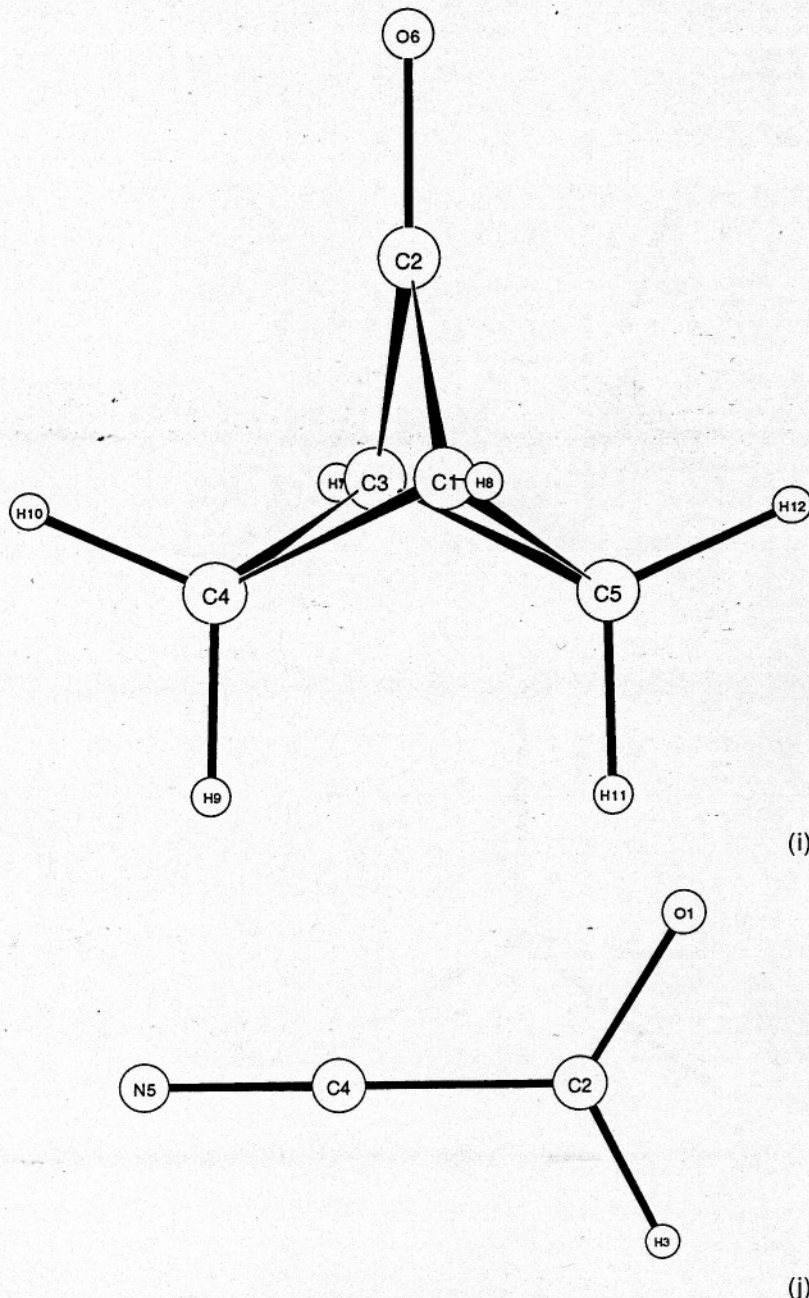


FIGURE 1. (Continued)

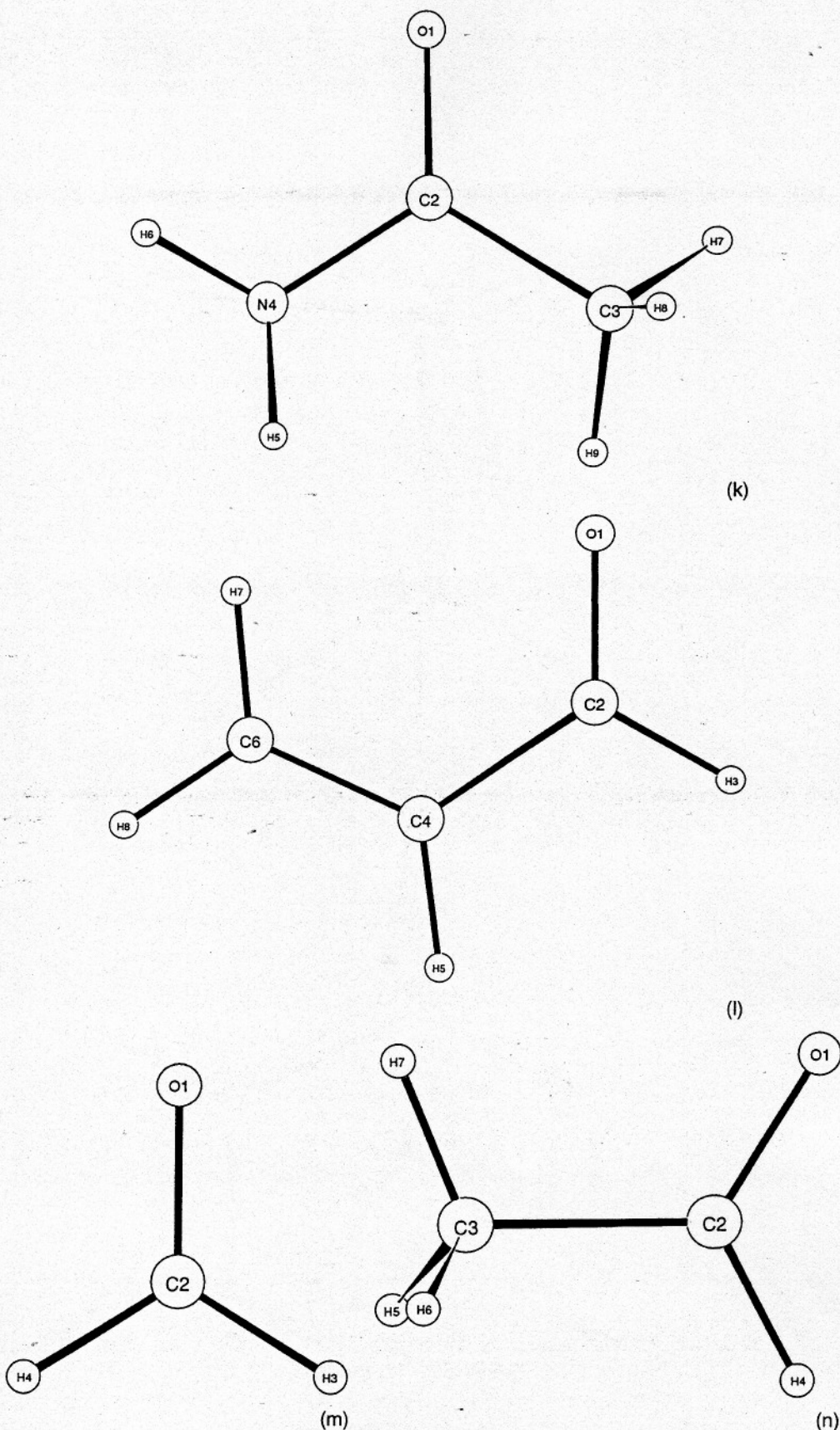
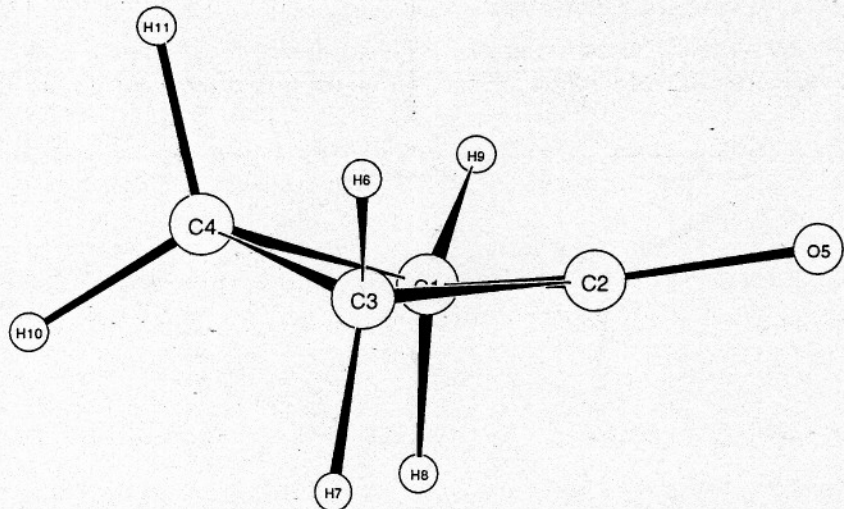
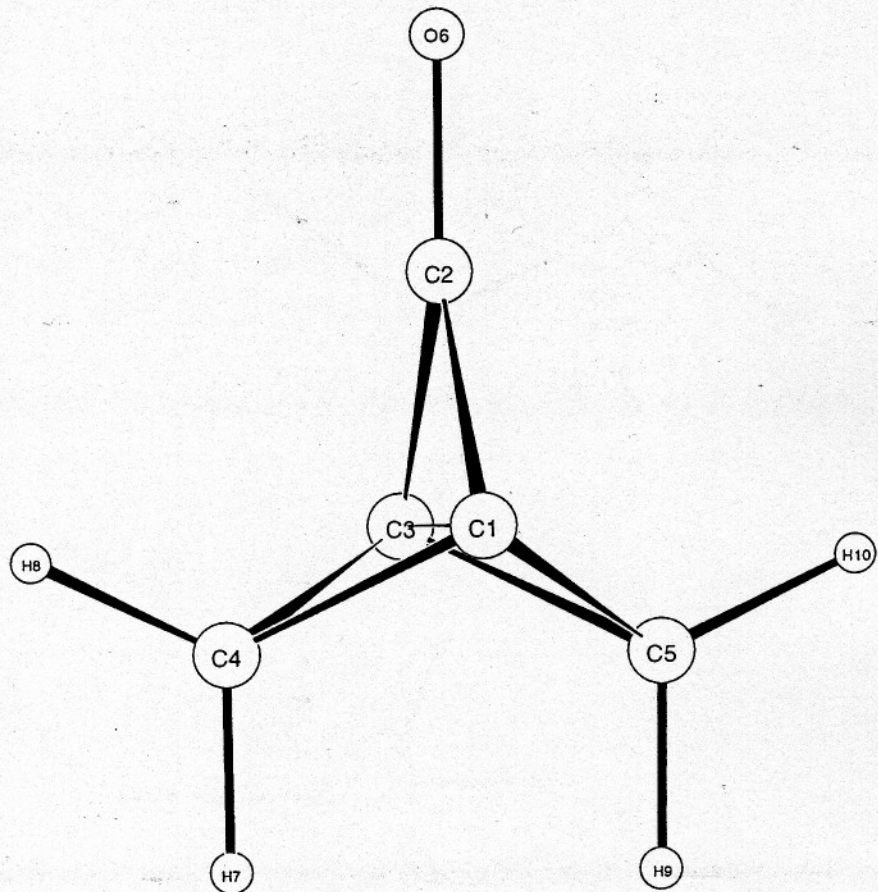


FIGURE 1. (Continued)



(o)



(p)

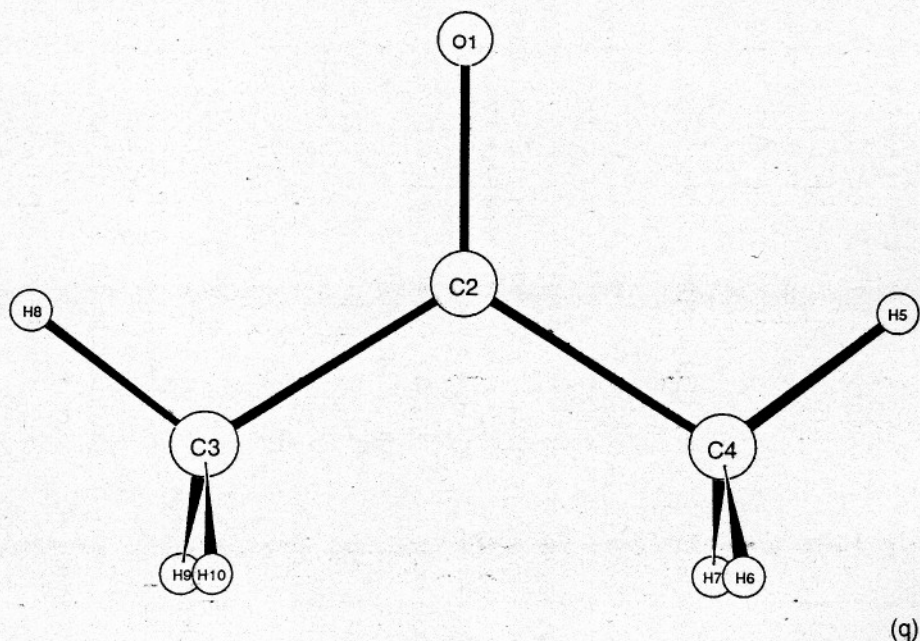
FIGURE 1. (Continued)

tematically change the shielding tensor to an extend that allows measured tensors to be used to probe local electronic structure?

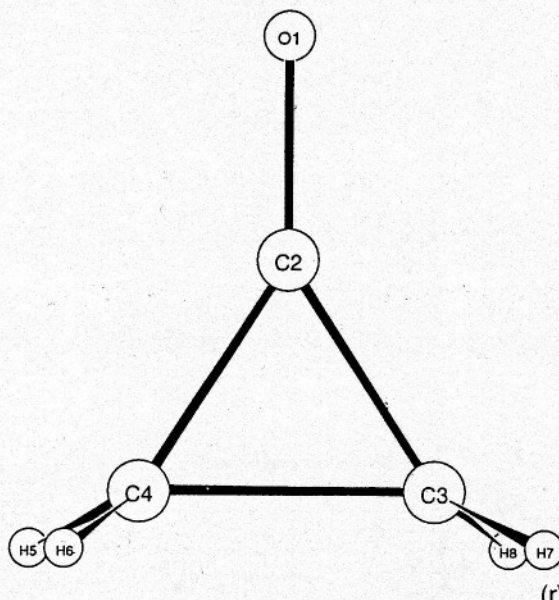
COMPUTATIONAL STRATEGY

A rather serious problem facing ab initio magnetic properties calculations is the inclusion of dynamic electron correlation. Simple SCF predictions can be achieved as a computational cost that

scales approximately as the cube of the number of atomic basis orbitals (N^3). In contrast, most correlated calculations such as second-order perturbation theory require effort scaling as N^5 (or higher). It was particularly for this reason we chose to examine the carbonyl functional group in this study; it has proven to be especially troublesome for SCF-level CST predictions because electron correlation plays such an important role [1]. In fact, for most molecules that contain multiple bonds



(q)



(r)

FIGURE 1. (Continued)

TABLE I
Optimized geometries and energies for all molecules using the TZP basis sets and MBPT(2) method.^a

Molecule	Symmetry	Energy	Optimized Geometrical Parameters
HO—CHO	C_s	−189.418 543	$r(C_2O_1) = 1.2058$, $r(C_2H_3) = 1.0930$, $r(C_2O_4) = 1.3509$, $r(O_4H_5) = 0.9713$, $a(O_1C_2H_3) = 125.52$, $a(O_1C_2O_4) = 125.03$, $a(C_2O_4H_5) = 106.29$
CH ₃ O—CHO	C_s	−228.614 623	$r(C_2O_1) = 1.2082$, $r(C_2H_3) = 1.0946$, $r(C_2O_4) = 1.3438$, $r(C_5O_4) = 1.4417$, $r(C_5H_8) = 1.0889$, $r(C_5H_6) = 1.0858$, $a(O_1C_2H_3) = 125.31$, $a(O_1C_2O_4) = 125.72$, $a(C_2O_4C_5) = 114.18$, $a(O_4C_5H_8) = 110.30$, $a(O_4C_5H_6) = 105.30$
Cl—CHO	C_s	−573.441 673	$r(C_2O_1) = 1.1908$, $r(C_2H_3) = 1.0934$, $r(C_2Cl_4) = 1.7775$, $a(O_1C_2H_3) = 126.58$, $a(H_3C_2Cl_4) = 109.83$
2-Cyclopropene-1-one	C_{2v}	−190.247 110	$r(C_2O_1) = 1.2067$, $r(C_2C_3) = 1.4390$, $r(C_3H_6) = 1.0808$, $r(C_3C_4) = 1.3561$, $a(C_3C_2C_4) = 56.22$, $a(C_2C_3H_6) = 154.20$
NH ₂ —CHO	C_1	−169.558 859	$r(C_2O_1) = 1.2173$, $r(C_2H_3) = 1.1002$, $r(C_2N_4) = 1.3670$, $r(N_4H_5) = 1.0090$, $r(N_4H_6) = 1.0067$, $a(H_3C_2O_1) = 122.97$, $a(N_4C_2O_1) = 124.71$, $a(H_5N_4C_2) = 117.88$, $a(H_6N_4C_2) = 119.54$, $d(H_5N_4C_2O_1) = 10.16$, $d(H_6N_4C_2H_3) = 13.90$
F—CHO	C_s	−213.413 961	$r(C_2O_1) = 1.1856$, $r(C_2H_3) = 1.0913$, $r(C_2F_4) = 1.3528$, $a(O_1C_2H_3) = 128.31$, $a(H_3C_2F_4) = 108.83$
CH ₃ COOH	C_s	−228.641 778	$r(C_2O_1) = 1.2105$, $r(C_2O_3) = 1.3618$, $r(O_3H_4) = 0.9707$, $r(C_2C_5) = 1.5020$, $r(C_5H_6) = 1.0861$, $r(C_5H_8) = 1.0900$, $a(H_4O_3C_2) = 105.60$, $a(O_3C_2O_1) = 122.57$, $a(O_3C_2C_5) = 111.06$, $a(C_2C_5H_6) = 109.50$, $a(C_2C_5H_8) = 109.57$, $d(H_7C_5C_2O_1) = 120.97$
CH ₃ COOCH ₃	C_s	−267.836 958	$r(C_2O_1) = 1.2123$, $r(C_2C_3) = 1.5047$, $r(C_3H_5) = 1.0868$, $r(C_3H_7) = 1.0900$, $r(C_2O_4) = 1.3553$, $r(O_4C_8) = 1.4388$, $r(C_8H_{10}) = 1.0890$, $r(C_8H_9) = 1.0865$, $a(O_1C_2O_4) = 123.40$, $a(O_1C_2C_3) = 126.10$, $a(C_2C_3H_5) = 109.41$, $a(C_2C_3H_7) = 109.69$, $a(C_2O_4C_8) = 114.28$, $a(O_4C_8H_{10}) = 110.49$, $a(O_4C_8H_9) = 105.27$, $d(H_7C_3C_2O_1) = 120.88$, $d(H_{10}C_8O_4C_2) = 60.49$
Bicyclo[1.1.1]pent-2-one	C_{2v}	−268.685 824	$r(C_2O_6) = 1.2012$, $r(C_2C_1) = 1.5344$, $r(C_1H_8) = 1.0870$, $r(C_1C_4) = 1.5641$, $r(C_4H_{10}) = 1.0905$, $r(C_4H_9) = 1.0914$, $a(O_6C_2C_1) = 140.56$, $a(C_2C_1H_8) = 130.09$, $a(C_1C_2C_3) = 78.88$, $a(C_1C_4C_3) = 77.10$, $a(C_1C_4H_{10}) = 117.68$, $a(C_1C_4H_9) = 113.77$, $d(C_2C_3C_1C_4) = 119.62$
NC—CHO	C_s	−206.343 401	$r(C_2O_1) = 1.2132$, $r(C_2H_3) = 1.0973$, $r(C_2C_4) = 1.4724$, $r(C_4N_5) = 1.1757$, $a(O_1C_2H_3) = 122.18$, $a(H_3C_2C_4) = 115.84$

NH ₂ COCH ₃	C ₁	-208.780 419	$r(C_2O_1) = 1.2215, r(C_3C_2) = 1.5149, r(C_2N_4) = 1.3752, r(N_4H_5) = 1.0069,$ $r(N_4H_6) = 1.0096, r(C_3H_7) = 1.0914, r(C_3H_8) = 1.0879, r(C_3H_9) = 1.0896,$ $a(O_1C_2N_4) = 122.79, a(N_4C_2C_3) = 114.87, a(C_2N_4H_5) = 119.79,$ $a(C_2N_4H_6) = 116.31, a(C_2C_3H_7) = 108.78, a(C_2C_3H_8) = 112.74,$ $a(C_2C_3H_9) = 108.61, d(N_4C_2O_1C_3) = 180.0, d(H_6N_4C_2O_1) = 13.11,$ $d(H_5N_4C_2O_1) = 163.77, d(H_7C_3C_2O_1) = 82.46, d(H_8C_3C_2O_1) = 34.93,$ $d(H_9C_3C_2O_1) = 156.78$
H ₂ C=CH—CHO	C _s	-191.495 703	$r(C_2O_1) = 1.2203, r(C_2H_3) = 1.1037, r(C_2C_4) = 1.4852, r(C_4H_5) = 1.0845,$ $r(C_4C_6) = 1.3399, r(C_6H_7) = 1.0836, r(C_6H_8) = 1.0824, a(O_1C_2H_3) = 120.32,$ $a(H_3C_2C_4) = 115.47, a(C_2C_4H_5) = 117.32, a(C_2C_4C_6) = 121.38,$ $a(C_4C_6H_8) = 121.53, a(C_4C_6H_7) = 120.08$
H ₂ CO	C _{2v}	-114.278 488	$r(C_2O_1) = 1.2143, r(C_2H_3) = 1.1013, a(H_4C_2H_3) = 116.21$
CH ₃ —CHO	C _s	-153.502 728	$r(C_2O_1) = 1.271, r(C_2H_4) = 1.1051, r(C_2C_3) = 1.5032, r(C_3H_5) = 1.0925,$ $r(C_3H_7) = 1.0881, a(O_1C_2H_4) = 120.17, a(O_1C_2C_3) = 124.39,$ $a(C_2C_3H_7) = 110.68, a(C_2C_3H_6) = 109.45, d(H_6C_3C_2O_1) = 121.41$
Cyclobutanone	C _s	-230.632 981	$r(C_2O_5) = 1.2074, r(C_2C_3) = 1.5361, r(C_3H_6) = 1.0918, r(C_3H_7) = 1.0942,$ $r(C_3C_4) = 1.5575, r(C_4H_{11}) = 1.0907, r(C_4H_{10}) = 1.0898, a(C_3C_2O_5) = 133.98,$ $a(C_1C_2C_3) = 91.74, a(C_2C_3C_4) = 86.95, a(C_3C_4C_1) = 90.12,$ $a(H_6C_3C_4) = 119.24, a(H_6C_3C_2) = 116.97, a(H_7C_3C_4) = 112.27,$ $a(H_7C_3C_2) = 110.17, a(H_{11}C_4C_3) = 111.64, a(H_{10}C_4C_3) = 116.41,$ $d(H_6C_3C_2O_5) = 37.11, d(H_7C_3C_2O_5) = 88.82, d(H_{11}C_4C_3H_6) = 21.31,$ $d(H_{10}C_4C_3H_7) = 24.64, d(C_4C_3C_2O_5) = 158.55$
Tricyclo[1.1.1.0 ^{1,3}]pent-2-one	C _{2v}	-267.440 618	$r(C_2O_6) = 1.1860, r(C_2C_1) = 1.5242, r(C_1C_3) = 1.6994, r(C_1C_4) = 1.5330,$ $r(C_4H_8) = 1.0845, r(C_4H_7) = 1.0846, a(O_6C_2C_1) = 146.12, a(C_1C_2C_3) = 67.77,$ $a(C_2C_1C_5) = 91.99, a(C_1C_4C_3) = 67.33, a(C_3C_4H_8) = 118.47,$ $a(C_1C_4H_7) = 114.01, d(C_4C_3C_1C_2) = 119.84$
CH ₃ COCH ₃	C _{2v}	-192.726 679	$r(C_2O_1) = 1.2204, r(C_2C_4) = 1.5137, r(C_4H_5) = 1.0881, r(C_4H_6) = 1.0924,$ $a(C_3C_2H_4) = 115.88, a(C_2C_3H_5) = 110.16, a(C_2C_4H_6) = 109.85,$ $a(O_1C_2C_4H_6) = 121.14$
Cyclopropanone	C _{2v}	-191.468 323	$r(C_2O_1) = 1.2049, r(C_2C_3) = 1.4703, r(C_3H_7) = 1.0839, r(C_3C_4) = 1.5776,$ $a(C_3C_2C_4) = 64.90, a(C_2C_3H_7) = 118.71, d(H_6C_4C_2O_1) = 74.50$

^a Energies are given in atomic units, bond distances are in angstroms, and bond angles as well as dihedral angles are in degrees.

adjacent to lone pairs of electrons, electron correlation has been found to be important for accurately determining the chemical shielding tensors. The π bonds have relatively low lying π^* molecular orbitals for which the $\pi \rightarrow \pi^*$ energy difference is small. The nonbonded lone pairs of electrons occupy high-lying molecular orbitals; as a result the energy difference between them and π^* orbitals can also be relatively small. As shown later, these small $n \rightarrow \pi^*$ orbital energy gaps strongly affect the computed CST and contribute strongly to dynamical correlation of the lone pair electrons, and thus must be accurately described.

Another factor which strongly influences the CST is the local hybridization and geometry about the carbon atom. As the molecule undergoes bending or stretching distortion, the chemical shielding responds to changes in the hybridization and electron density. Bond stretching distortions, in particular, can also significantly modulate the energy gaps between occupied and unoccupied orbitals. The inclusion of atomic basis functions, which have adequate angular and radial flexibility to "track" such changes in hybridization and orbital energies, is thus critical.

SERIES OF CARBONYL COMPOUNDS STUDIED

Experimentalists have the difficult task of inferring the structure changes (i.e., during vibrations, due to ring strain or steric repulsion, or in response to solvation or to impurities in a solid-state lattice) that correspond to measured CST changes. By investigating several specific prototype examples of how the CST changes with addition of *substituents* or *geometry distortion*, we hope to better understand the nature of the shielding variation among families of compounds. The unsubstituted and unstrained formaldehyde molecule H_2CO forms the reference point with respect to which other aldehydes and ketones are compared. Specifically, we have looked at cyclic ketones including cyclopropanone as well as larger ring systems with less strain at the carbonyl carbon. Also, we attached various functional groups to our prototypical unsubstituted molecule, formaldehyde. Finally, we examined (realistically and extremely) geometrically twisted and bond-stretched formaldehyde to study how the CST responds to hybridization changes and deformations over a very wide range.

Computational Considerations

We used the ACES II [2] and GAUSSIAN-94 [3] programs to calculate electronic energies and shieldings and to optimize geometries. The shielding tensors were calculated at the MBPT(2), SCF, and DFT levels of theory using gauge including atomic orbitals (GIAOs). In addition, the shielding tensors were symmetrized before the diagonalization step. We used three different types of atomic orbital basis sets: Dunning's TZP basis sets [4] for molecular energies and geometries, the Schafer et al. basis sets [5] for magnetic properties, and Dunning's large cc-pVTZ basis sets [6] also for magnetic properties. All of these basis sets include polarization functions.

All geometries were optimized at the MBPT(2) level using the TZP basis, and each of the struc-

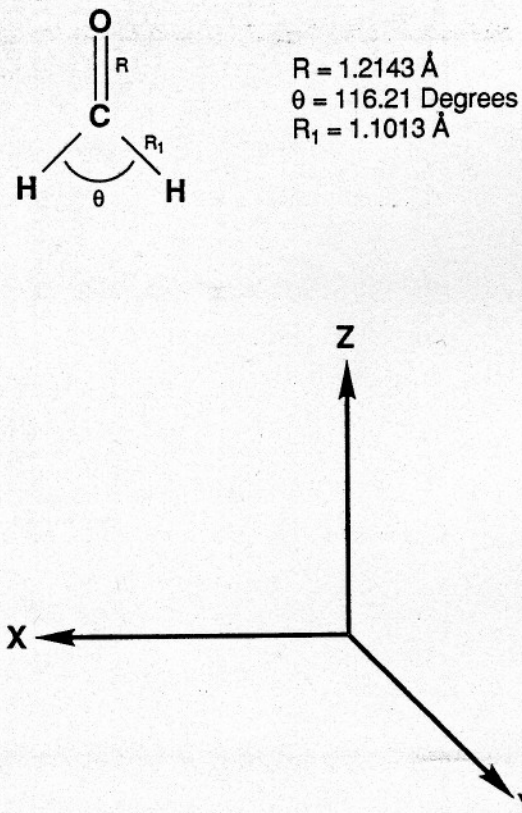


FIGURE 2. Formaldehyde equilibrium geometry and orientation with respect to the Cartesian axes.

tures reported below in Figure 1 and Table I was the lowest energy structure we could find on the ground-state potential energy surface. The ACES II program with Ahlrichs's TZP bases and Dunning's cc-pVTZ bases were used for the SCF and MBPT(2) shielding tensor calculations. For the DFT shielding calculations we used GAUSSIAN-94, the B3LYP functional, Ahlrichs's TZP basis, and Dunning's cc-pVTZ bases. The TZP basis sets were used to generate insight with regard to the experimental results, and the cc-pVTZ basis sets were used to minimize the basis set incompleteness and give a better comparison of current theoretical methods. In addition, the GAMESS [7] package was used to calculate the multiconfiguration self-consistent-field (MCSCF) wave functions for molecules we suspected to have significant multiconfigurational character. In all of our calculations, the full set of Cartesian polarization functions was used.

Findings and Discussion

ROLE OF LOW-ENERGY SINGLY EXCITED STATES IN SHIELDING TENSOR ELEMENTS

The chemical shielding tensor of a nucleus N can be expressed as a sum of two components [8], the paramagnetic contribution σ_N^p and the diamagnetic contribution σ_N^d . The paramagnetic term is given in terms of a sum over excited electronic states $|n\rangle$:

$$\sigma_N^p = \frac{\mu_0 e^2}{8\pi m^2} \sum_{n \neq 0} \frac{\langle o | \sum_j \frac{1_{jN}}{r_{jN}^3} | n \rangle \langle n | \sum_j 1_j | o \rangle + \langle o | \sum_j 1_j | n \rangle \langle n | \sum_j \frac{1_{jN}}{r_{jN}^3} | o \rangle}{E_0 - E_n} \quad (1)$$

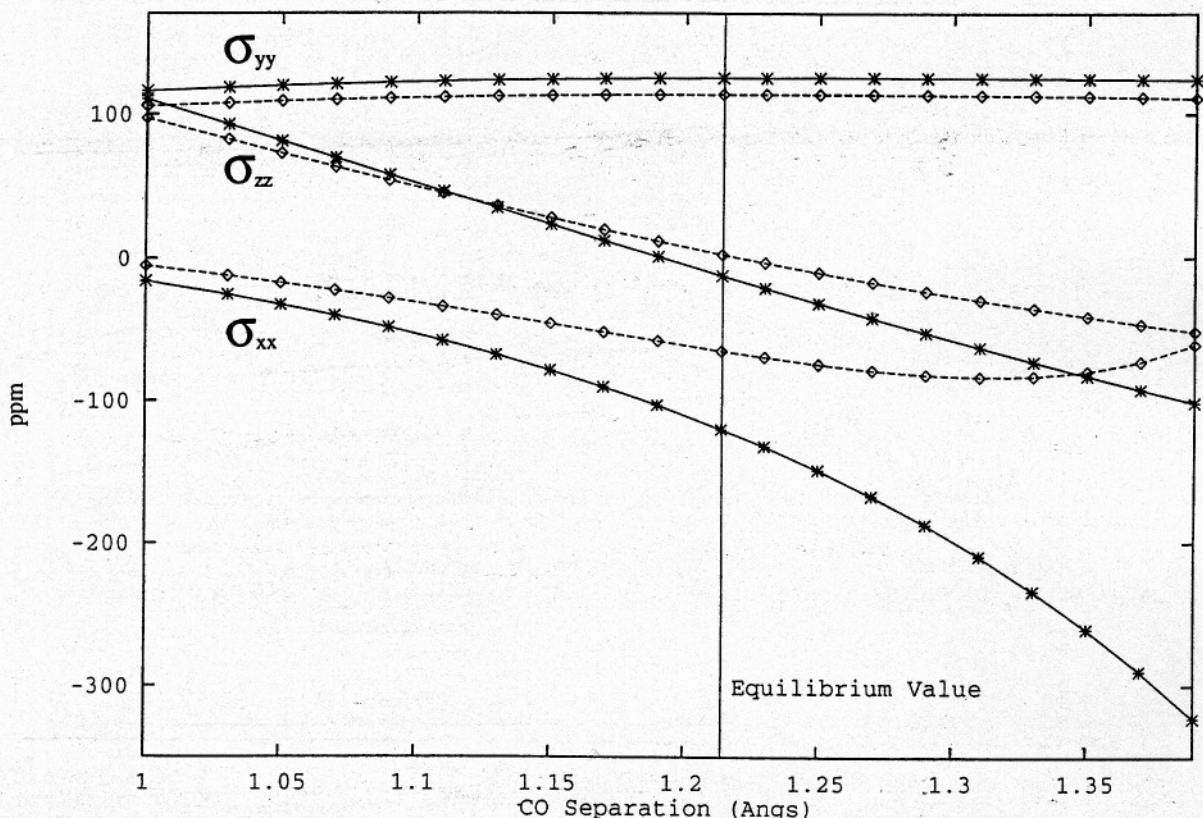


FIGURE 3. Formaldehyde shieldings as a function of CO distance. Solid lines with stars show the SCF shielding while the MBPT(2) shieldings are given by dashed lines with open diamonds.

while the diamagnetic component is an average value over the ground electronic state $|o\rangle$:

$$\sigma_N^d = \frac{\mu_0 e^2}{8\pi m} \langle o | \sum_j \frac{\mathbf{r}_j \mathbf{r}_{jN} - \mathbf{r}_j \mathbf{r}_{jN}}{r_{jN}^3} | o \rangle \quad (2)$$

In both equations the sum j runs over electrons whose angular momentum and distance relative to the nucleus N are \mathbf{l}_{jN} and \mathbf{r}_{jN} , respectively, and over electrons whose angular momentum and distance relative to the gauge origin of the vector potential are \mathbf{l}_j and \mathbf{r}_j , respectively.

The dependence of the tensor elements of σ_N^p on the molecular geometry can best be described by considering the structure of Eq. (1). Geometric changes that substantially modify the energies of singly excited states (because the angular momentum operators $\mathbf{l}_N | r_N^3$ and \mathbf{l} are one-electron operators) can effect major changes in σ_N^p , especially if they cause one or more energy gaps, $E_0 - E_n$, to become small.

Given that the ground states of all the species studied here are of singlet spin and totally symmetric spatial symmetry, the symmetries of the excited states $|n\rangle$ that can affect various components of σ_N^p can be inferred based on the symmetries of $\mathbf{l}_N | r_N^3$ and of \mathbf{l} . Clearly, the i, k component of $\sigma_{N,i,k}^p$ ($i, k = X, Y, \text{ or } Z$) can be nonzero if and only if the symmetry of the excited state $|n\rangle$ matches both the symmetry of the i th component of $\mathbf{l}_N | r_N^3$ and the symmetry of the k th component of \mathbf{l} .

For example, in the C_{2v} symmetry of formaldehyde, $|o\rangle$ is of 1A_1 symmetry and for the ${}^{13}\text{C}$ nucleus $\mathbf{l}_N | r_N^3$ and \mathbf{l} have symmetries $X_{b_2} \otimes Y_{b_1} = a_2$, $Y_{b_1} \otimes Z_{a_1} = b_1$, and $X_{b_2} \otimes Z_{a_1} = b_2$. Thus, only low-lying singly excited states of a_2 , b_1 or b_2 symmetry can contribute to the ${}^{13}\text{C}$ σ_N^p through matrix elements in the numerator of Eq. (1). The nature of the numerator in Eq. (1) zeroes off-diagonal terms when the three Cartesian axes transform under three different irreducible repre-

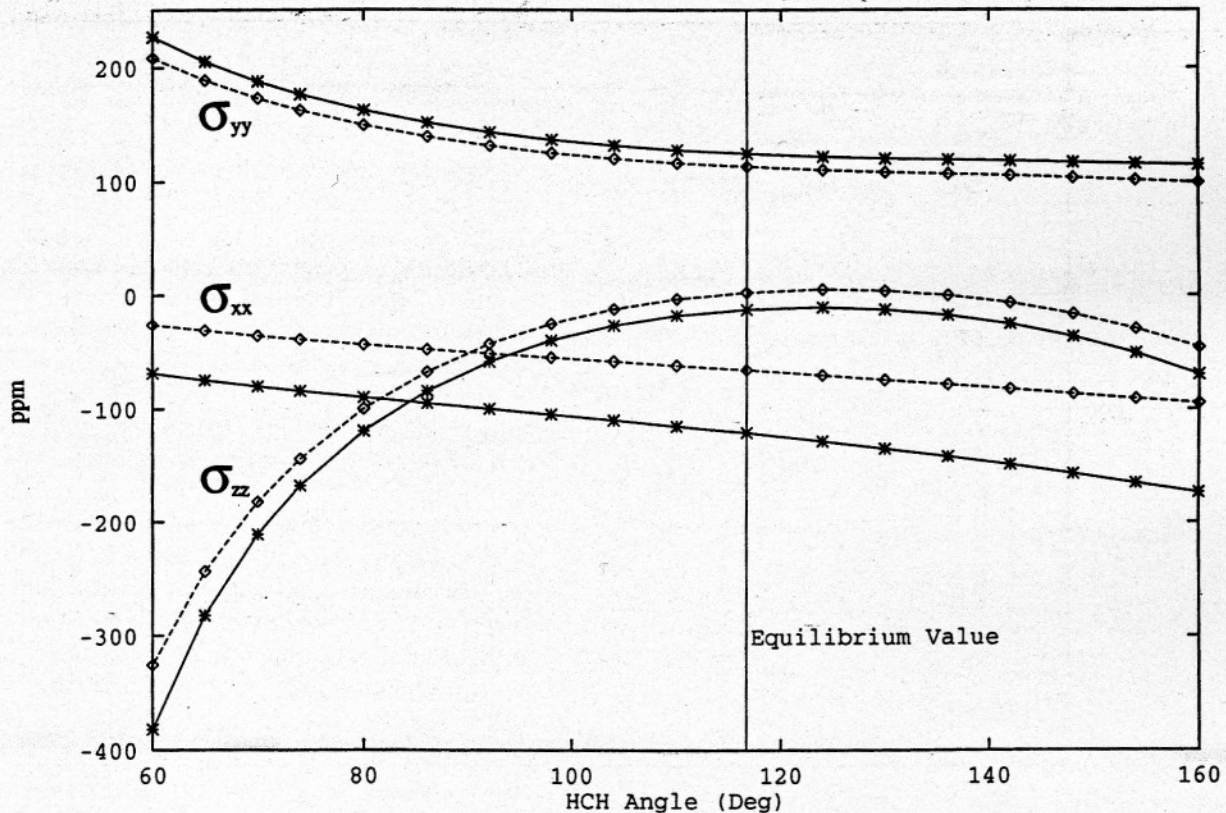


FIGURE 4. Formaldehyde shieldings as a function of HCH angle. Solid lines with stars show the SCF shielding while the MBPT(2) shieldings are given by dashed lines with open diamonds.

sentations because no $|n\rangle$ exists that makes both portions of the matrix element nonzero. Symmetry also dictates that the diamagnetic component of the shielding (σ_N^d) is diagonal whenever X, Y, and Z transform as different irreducible representations as in C_{2v} symmetry.

Thus, we expect the ^{13}C σ_N to be diagonal when C_{2v} symmetry or higher holds, and we expect geometry induced changes in σ_{xx} , σ_{yy} , and σ_{zz} components to be largest when distortions strongly modify the energies of a low-lying excited states of $^1\text{B}_1$, $^1\text{B}_2$, or $^1\text{A}_2$ symmetry. Ketones and aldehydes have low energy $n_{b_1} \rightarrow \pi_{b_1}^*$ ($^1\text{A}_2$), $n_{a_1} \rightarrow \pi_{b_1}^*$ ($^1\text{B}_1$), and $\pi_{b_1} \rightarrow \pi_{b_1}^*$ ($^1\text{A}_1$) excited states with $E_0 - E_n$ values generally increasing in the above order. Among vibrations which preserve C_{2v} symmetry, it is primarily the C=O stretch that strongly affects the energy differences of the

excitations because it modifies the energies of the π_{b_1} and $\pi_{b_1}^*$ orbitals. Therefore, we anticipate that the diagonal σ_{xx} and σ_{zz} components of σ_N should vary strongly with C=O distances, while σ_{yy} should vary less strongly. This expectation is verified below.

For vibrations that destroy C_{2v} symmetry (e.g., asymmetric HCH stretching motion or out of plane HCH puckering) more significant variations in σ_{yy} can occur because at least one of the $^1\text{A}_2$, $^1\text{B}_1$, or $^1\text{A}_1$ low-energy excited states becomes the proper symmetry to permit mixing (i.e., $^1\text{A}_1$ and $^1\text{B}_2$ mix under HCH asymmetric stretching and $^1\text{A}_2$ and $^1\text{B}_2$ mix under HCH puckering). Of these two distortions, the HCH puckering would be expected to produce the strongest change in σ_{yy} because this distortion more strongly alters the π and π^* orbital energies.

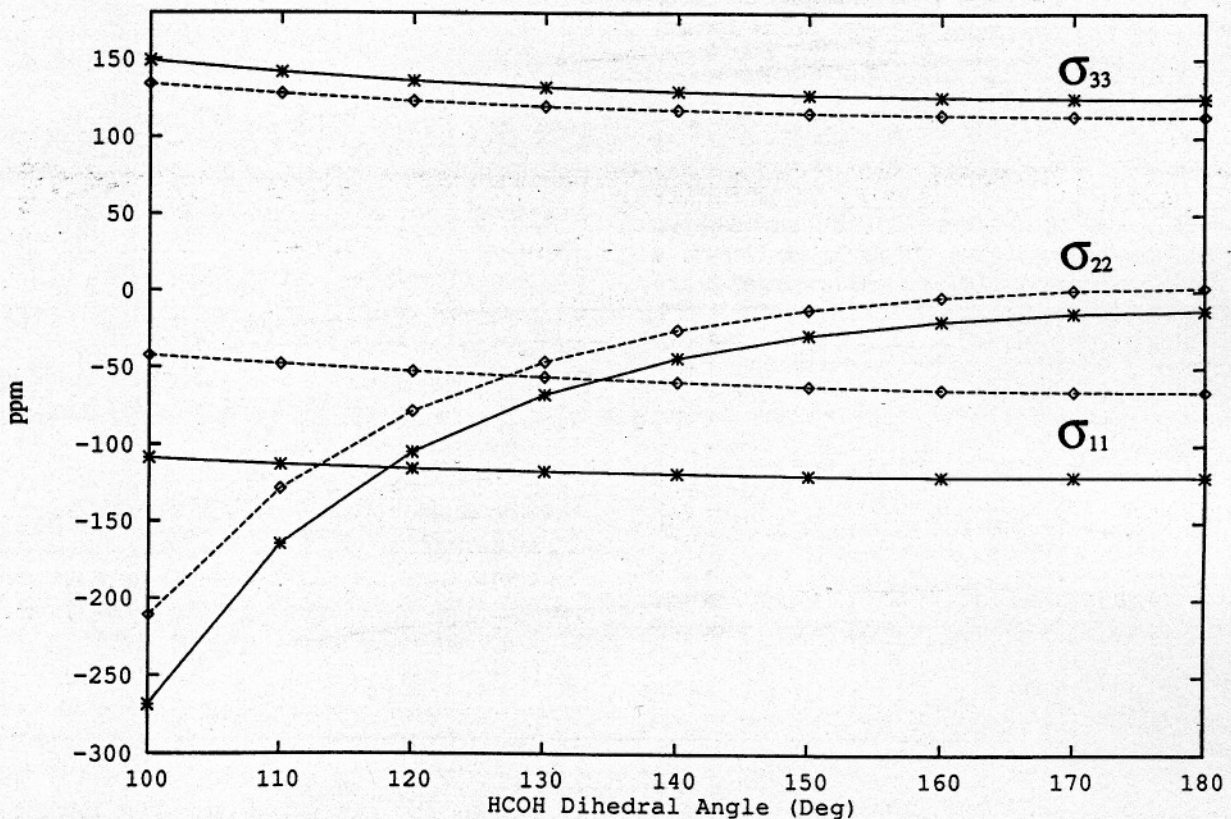


FIGURE 5. Formaldehyde shieldings as a function of HCOH dihedral angle. Since this is a C_{2v} symmetry breaking distortion, we use σ_{11} , σ_{22} , and σ_{33} to label the eigenvalues of the diagonalized shielding tensor. Solid lines with stars show the SCF shielding while the MBPT(2) shieldings are given by dashed lines with open diamonds.

SCF AND MBPT(2) SHIELDINGS OF ARTIFICIALLY DISTORTED FORMALDEHYDE

We calculated the SCF and MBPT(2) shielding tensors for the reference molecule formaldehyde's carbon atom at a variety of geometries representing both small and "severe" changes in CO bond length, HCH bond angle, HCOH dihedral angle, and HCH asymmetric stretch. For each deformation, all remaining internal degrees of freedom were fixed at the minimum energy values shown in Figure 2. The primary findings of these numerical experiments are:

1. CO Bond Length Variation

The three eigenvalues of the CST at various CO bond lengths are shown in Figure 3 for the SCF and MBPT(2) levels of theory. Note that the out-

of-plane σ_{yy} component remains relatively constant over a wide range of distortion and that the variations of the SCF and MBPT(2) predictions are quite similar for this component. The σ_{xx} and σ_{zz} components vary more strongly with distortion and the SCF-MBPT(2) difference becomes pronounced as the CO bond is stretched (but not compressed). Both of these features are consistent with the analysis given above. Finally, the slopes of the SCF σ_{xx} and σ_{zz} are larger in magnitude than are the MBPT(2) slopes, indicating that the SCF treatment tends to exaggerate the bond length dependence.

2. HCH Bending Variation

Figure 4 shows the dependence of the shielding tensor eigenvalue on the HCH bond angle. For this

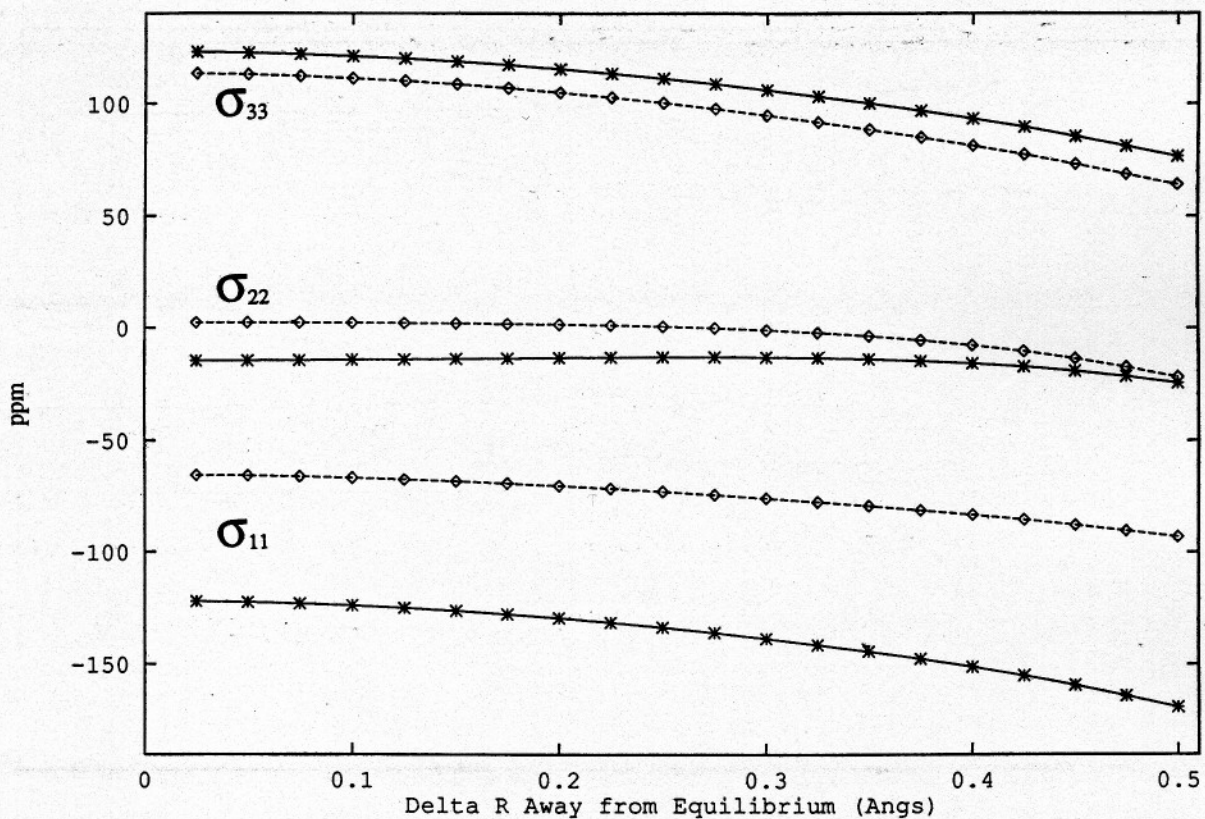


FIGURE 6. Formaldehyde shieldings as a function of HCH asymmetric stretch. This is also a symmetry breaking motion, so we use σ_{11} , σ_{22} , and σ_{33} to label the eigenvalues. Solid lines with stars show the SCF shielding while the MBPT(2) shieldings are given by dashed lines with open diamonds.

distortion, again the σ_{zz} component changes most dramatically; yet for all three components, the SCF and MBPT(2) results track one another closely but with appreciable systematic differences.

3. HCOH Dihedral Angle Variation

Figure 5 shows the dependence of the shielding tensor on the HCOH dihedral angle. This type of distortion, which moves the two hydrogen atoms out of the molecular plane, destroys one of the C_{2v} mirror planes and lowers the molecular symmetry to C_s symmetry. The shielding tensor for the carbonyl carbon is no longer diagonal in the Cartesian frame because two of the three components transform under the same irreducible representation. We have therefore diagonalized the tensor and plotted the eigenvalues σ_{33} , σ_{22} , and σ_{11} with the condition that $\sigma_{33} \geq \sigma_{22} \geq \sigma_{11}$. We see from Figure 5 that again σ_{22} , which corresponds to σ_{zz} in C_{2v} symmetry, drops significantly when the dihedral angle is reduced below 140°, but the other two eigenvalues vary less strongly.

4. HCH Asymmetric Stretch Variation

In Figure 6, we show the shielding as a function of HCH asymmetric stretch. This type of distortion also destroys one of the C_{2v} mirror planes and lowers the molecular symmetry to C_s symmetry. We have diagonalized the shielding tensor and plotted the resulting eigenvalues as described above. Even for our largest distortion 0.5 Å, the asymmetric stretch does not effect the chemical shielding very strongly.

All of the above findings on the prototype reference molecule H₂CO indicate that (1) SCF-MBPT(2) chemical shielding tensor component differences are large, but rather geometry independent although for CO bond length variation, the SCF treatment tends to exaggerate the rate of change of σ_{ii} and (2) the dynamic range of variation in CST values as geometry varies can be quite large (more than 100 ppm). These observations suggest that correlated CST calculations at equilibrium geometries followed by SCF-level treatment at nearby geometries with the addition of the correlation "correction" to the tensor components should give acceptable correlated chemical shielding tensors even for carbonyl CST values.

ELECTRON-DONATING AND -WITHDRAWING FUNCTIONAL GROUPS

To further understand the shielding at the carbonyl carbon, we performed calculations on a series of compounds that contain either an electron-withdrawing or electron-donating group adjacent to the carbonyl carbon. From the data presented in Table II and summarized in Figure 7, we observe that once again, the σ_{22} component (corresponding to σ_{zz} in C_{2v} symmetry) is the most sensitive to the electron-withdrawing or -donating groups. This is consistent with the model given above because σ_{zz} involves matrix elements of 1_z and $1_{Nz} | r_N^3$, which in turn, each have a_2 local symmetry. The lowest ($n_{b_2} \rightarrow \pi_{b_1}^*$) 1A_2 excited state has this symmetry, and this state's energy is altered by substitutions which affect the energy of the $\pi_{b_1}^*$ orbital.

In Figure 7 we have plotted the three principle components of the shielding tensor for all molecules at the SCF and MBPT(2) levels of theory such that the strongly varying σ_{22} component decreases monotonically from left to right when treated at the MBPT(2) level. Some general trends

TABLE II
Symmetrized MBPT(2) shieldings using the TZP basis sets at the calculated minimum energy structures for all 18 carbonyl-containing molecules

Molecule	σ_{11}	σ_{22}	σ_{33}
HO—CHO	-56.69	88.21	91.59
CH ₃ O—CHO	-55.01	84.79	85.97
Cl—CHO	-55.49	83.95	91.66
2-Cyclopropene-1-one	-65.51	77.36	138.53
NH ₂ —CHO	-52.95	72.95	106.41
F—CHO	-57.13	71.55	132.20
CH ₃ COOH	-65.98	69.40	85.71
CH ₃ COOCH ₃	-62.26	66.10	80.42
Bicyclo[1.1.1]pent-2-one	-91.45	65.44	73.16
NC—CHO	-55.24	61.45	110.31
NH ₂ COCH ₃	-55.90	46.48	104.36
CH ₂ =CH—CHO	-66.51	13.55	108.76
H ₂ CO	-65.45	2.33	113.39
CH ₃ —CHO	-78.43	0.63	110.09
Cyclobutanone	-78.34	-10.47	96.20
Tricyclo[1.1.1.0 ^{1,3}]pent-2-one	-79.12	-22.85	131.90
CH ₃ COCH ₃	-75.55	-24.60	111.56
Cyclopropanone	-63.36	-62.94	123.02

are noted clearly: molecules on the left side of Figure 7 have functional groups with sigma electron-withdrawing characteristics at the carbonyl carbon, while molecules on the right side show sigma electron-donating characteristics. Once again, the SCF and MBPT(2) data track one another but with significant *systematic* differences.

COMPARISON TO EXPERIMENTAL DATA

Because experimental *tensors* are derived from powder or single-crystal measurements and not from the gaseous or liquid states, much effort is required to extract the tensor components from NMR experiments. As a result, only a handful of the molecules studied in this work have also had their chemical shielding tensors determined experimentally. The use of external references such as tetramethylsilane (TMS) in NMR experiments also

complicates the comparison of theoretical shieldings and experimental shift tensors because the *absolute* shielding for the TMS molecule also needs to be computed. Jameson and Jameson [9] have proposed a relationship between the computed CH_3 shielding and the TMS shielding: $\text{TMS} = \text{CH}_4 - 7 \text{ ppm}$, which then requires one to compute the absolute shielding of the smaller CH_4 molecule.

Table III shows our chemical shieldings as chemical shifts where we compare them to the experimental shift tensors for six molecules. Our correlated MBPT(2) results for two of the three tensor elements compare as favorably (i.e., $\pm 5 \text{ ppm}$) to the experimental data as those obtained [1] earlier for noncarbonyl species. However, the computed δ_{22} element, which derives from the σ_{22} element found earlier in this study to be the most geometry and substituent sensitive, is systematically smaller than the experimental values by *much*

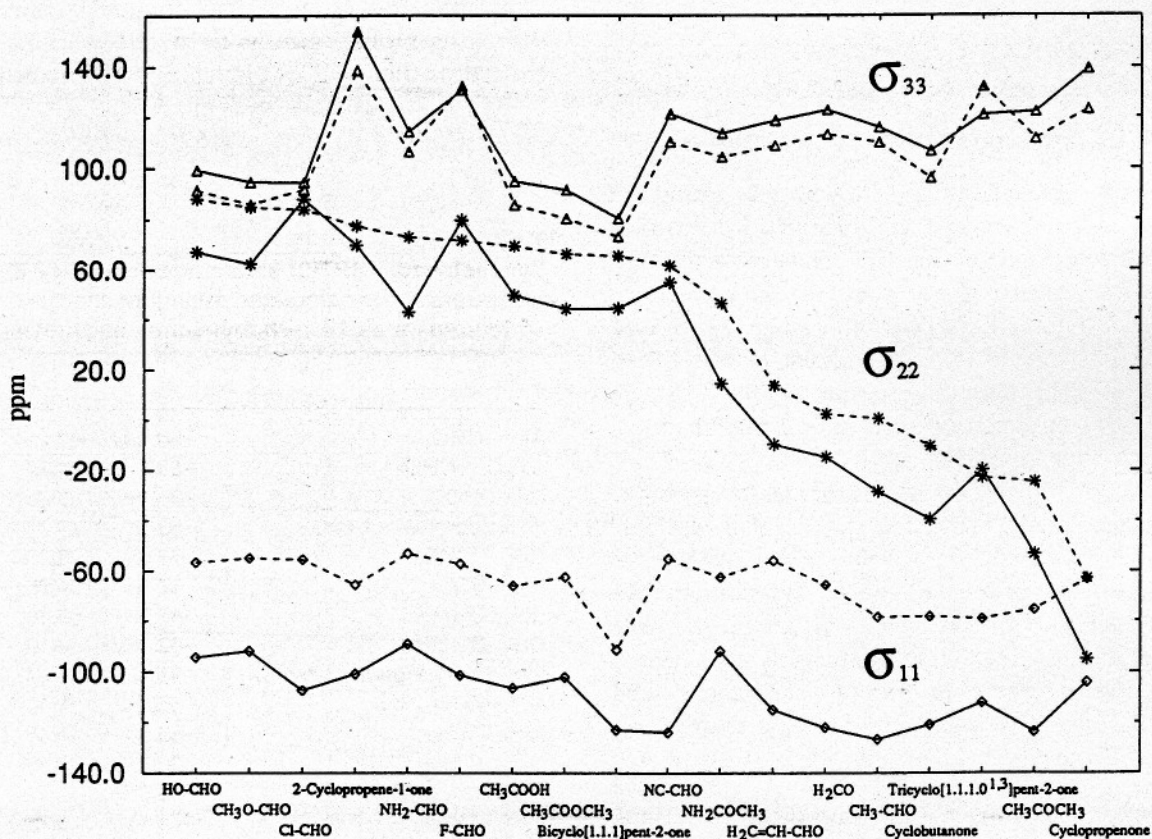


FIGURE 7. SCF and MBPT(2) chemical shielding tensor eigenvalues for 18 carbonyl-containing species. SCF shieldings are solid lines while MBPT(2) shieldings are given by dashed lines. The σ_{11} component is represented by triangles, the σ_{22} component by stars, and the σ_{33} component by diamonds.

TABLE III
Experimental and theoretical chemical shifts using tetramethylsilane (TMS) as the reference.^a

Molecule	Method	δ_{11}	δ_{22}	δ_{33}	δ_{iso}	$\Delta \delta_{iso}$
$\text{CH}_3\text{—CHO}$	Expt. [10]	276	234	87	200	
	MBPT(2)	274	195	86	185	15
	B3LYP	302	237	91	210	-10
CH_3COCH_3	Expt. [10]	279	265	79	208	
	MBPT(2)	272	221	84	192	16
	B3LYP	299	252	85	212	-4
HCOOH	Expt. [10]	251	162	92	168	
	MBPT(2)	253	108	104	155	13
	B3LYP	272	121	104	166	2
CH_3COOH	Expt. [10]	269	184	110	188	
	MBPT(2)	262	127	110	166	22
	B3LYP	282	141	111	178	10
HCOOCH_3	Expt. [10]	253	136	107	165	
	MBPT(2)	251	111	110	157	8
	B3LYP	270	124	111	168	-3
$\text{CH}_3\text{COOCH}_3$	Expt. [10]	267	160	120	182	
	MBPT(2)	258	130	116	168	14
	B3LYP	278	145	116	180	2

^a The theoretical shielding tensors are converted to chemical shift tensors by using $\delta_{ii} = \sigma_{\text{TMS}} - \sigma_{ii}$ and Jameson's method; $\sigma_{\text{TMS}} = \sigma_{\text{CH}_4} - 7$ ppm. MBPT(2) gives $\sigma_{\text{TMS}} = 196$ ppm, whereas the B3LYP method gives $\sigma_{\text{TMS}} = 185$ ppm. σ_{iso} is one-third the trace of δ and $\Delta \delta_{iso}$ is the deviation from the experimental value.

larger amounts (ca. 20–50 ppm). Because the methods we use do so well, for all compounds, on δ_{11} and δ_{33} , we believe it unlikely that the large discrepancies found in δ_{22} are entirely the result of errors in the theoretical treatment. We believe some of the differences in δ_{22} are due to the intermolecular interactions present in the solid which are not treated in our gas phase calculations. Shown in Figures 8(a) and 8(b) are data, including several compounds studied here, that amplify the claim that MBPT(2)-level (isotropic) chemical shifts agree better with experimental data than do SCF-level shifts.

WHAT ABOUT DENSITY FUNCTIONAL THEORY'S ABILITY TO PREDICT SHIELDINGS?

Because DFT has enjoyed remarkable success in recent years in predicting relative energies and geometries of molecules with better cost effective-

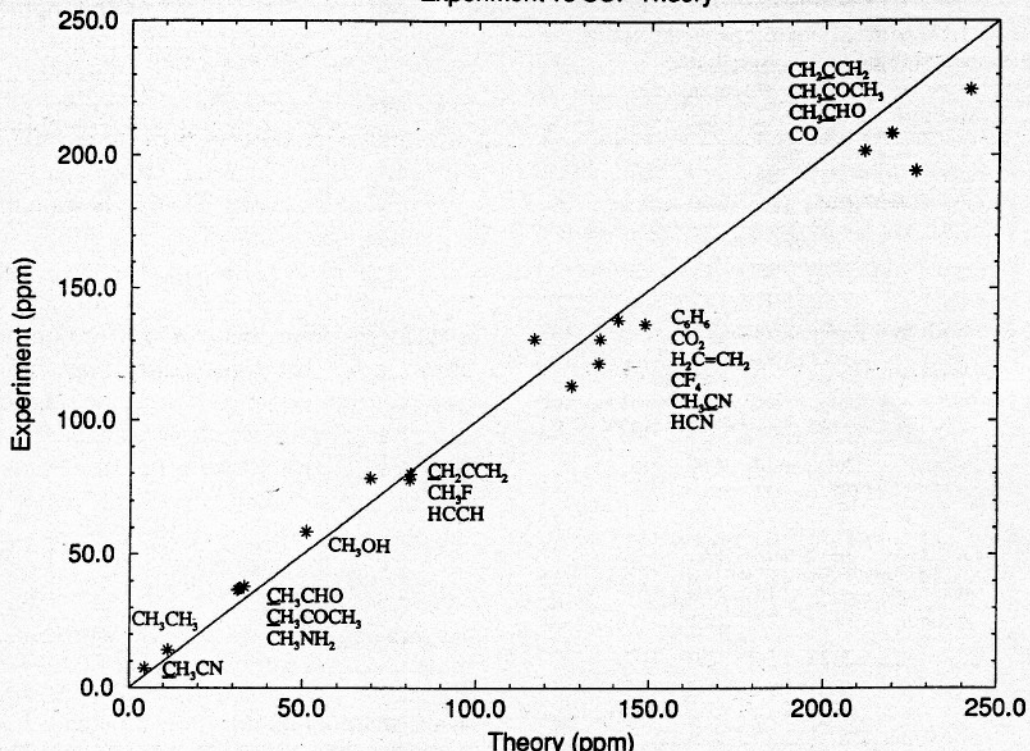
ness than conventional correlated methods, we decided to examine DFT shieldings in comparison with our SCF and MBPT(2) shieldings for the kinds of molecules studies here. Figure 9 and Table IV show how the B3LYP, SCF, and MBPT(2) shieldings compare for a range of molecules containing electron-withdrawing or electron-donating groups. Although the general trends indicate that DFT shieldings are not absurd, it seems the DFT values track neither the SCF nor the MBPT(2) results in a reliable manner for carbonyl-containing species, although B3LYP gives better (when compared to the experimental data) isotropic shifts (δ_{iso}) than the other two methods, as detailed also in Table III. These inconsistencies in the DFT-level predictions indicate that further work is needed before

TABLE IV
The three eigenvalues and one-third the trace σ_{iso} of the chemical shielding tensor for the carbonyl carbon are given at the SCF, MBPT(2), and B3LYP levels of theory for selected molecules.^a

Molecule	Method	σ_{11}	σ_{22}	σ_{33}	σ_{iso}
HO—CHO	SCF	-94	67	95	23
	MBPT(2)	-60	84	88	38
	B3LYP	-91	61	76	16
F—CHO	SCF	-100	75	130	35
	MBPT(2)	-60	67	129	45
	B3LYP	-94	53	110	23
H_2CO	SCF	-122	-14	119	-6
	MBPT(2)	-71	-6	110	11
	B3LYP	-113	-45	96	-20
$\text{CH}_3\text{—CHO}$	SCF	-126	-25	112	-13
	MBPT(2)	-81	-13	107	4
	B3LYP	-121	-47	89	-26
$\text{H}_2\text{C}=\text{CH}_2$	SCF	-78	86	179	62
	MBPT(2)	-45	87	180	74
	B3LYP	-75	62	167	51
CH_3CH_3	SCF	180	180	191	184
	MBPT(2)	184	184	197	188
	B3LYP	168	168	183	173
CH_4	SCF	195	195	195	195
	MBPT(2)	201	201	201	201
	B3LYP	189	189	189	189

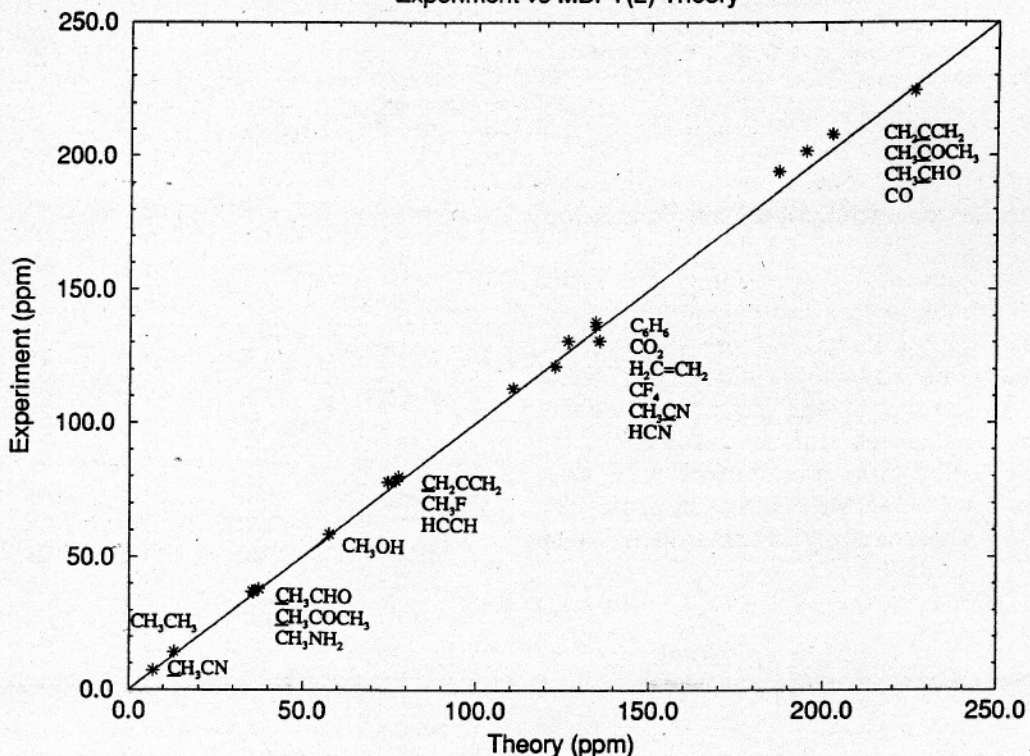
^a We used the cc-p VTZ basis sets in these shielding comparisons to minimize basis-set inadequacies and highlight differences between the methods. All molecules were optimized using the MBPT(2) method and the TZP basis sets. Small hydrocarbons are included to gauge the accuracy of these methods.

Experiment vs SCF Theory



(a)

Experiment vs MBPT(2) Theory



(b)

FIGURE 8. (a) Chemical shifts compared (SCF) vs. measures for a wide range of species. (b) Chemical shifts computed (MBPT(2)) vs. measures for a wide range of species.

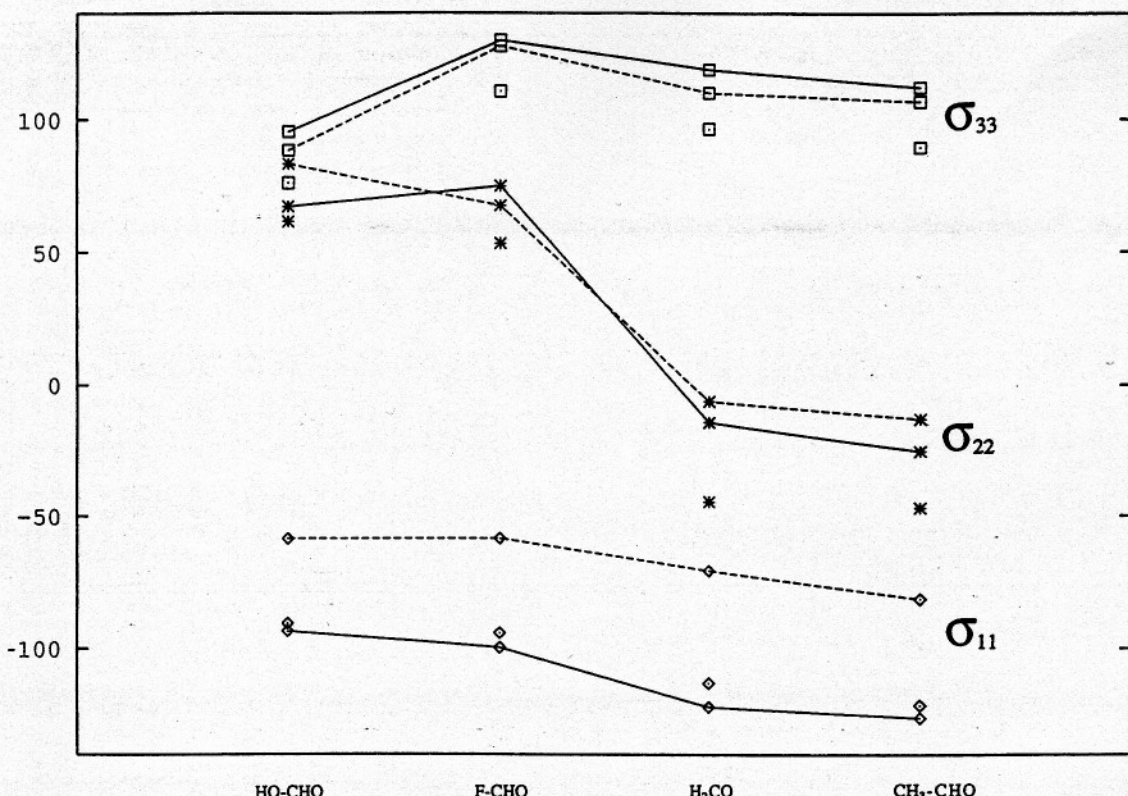


FIGURE 9. SCF, MBPT(2), and DFT shieldings for HO—CHO, F—CHO, H₂CO, and CH₃—CHO. The solid lines represent the SCF tensor components while the dashed lines represent the MBPT(2) tensor components. The data without lines corresponds to the DFT tensor components. Open squares denote σ_{33} values for each method, stars for σ_{22} values, and diamonds for σ_{11} values.

DFT shielding tensor components can be calibrated well enough to be of great use.

Conclusions

Our findings on the prototype reference molecule H₂CO and on 17 other carbonyl species indicate that (1) the SCF and MBPT(2) shielding tensors are substantially different, but, these differences are systematic and rather geometry independent and (2) the dynamic range of variation in CST values as the geometry varies can be quite large (more than 100 ppm). These factors suggest that SCF-level treatment of the CST with a constant correlation contribution added should be acceptable for analyzing the shielding as a function of geometrical distortion except perhaps for CO bond length variation, the effect in which SCF tends to exaggerate. We find that the σ_{11} and σ_{33} components of the CST computed at the MBPT(2)

level agree well (± 5 ppm) with experimental results. However, the σ_{22} components deviate much more (~ 20 –50 ppm). A DFT treatment or correlation does not produce systematically consistent accuracy in all three elements of σ but seems to do well on isotropic chemical shifts.

ACKNOWLEDGMENTS

This work was supported by the Office of Naval Research and by National Science Foundation Grant No. CHE91-16286.

References

1. J. Gauss, *J. Chem. Phys.* **99**, 3629 (1993).
2. J. F. Stanton, J. Gauss, J. D. Watts, W. J. Lauderdale, and R. J. Bartlett, *Int. J. Quant. Chem. Symp.* **26**, 879 (1992).
3. M. J. Frisch, G. W. Trucks, H. B. Schlegel, P. M. W. Gill, B. G. Johnson, M. A. Robb, J. R. Cheeseman, T. Keith, G. A. Petersson, J. A. Montgomery, K. Raghavachari, M. A.

- Al-Laham, V. G. Zakrzewski, J. V. Ortiz, J. B. Foresman, J. Cioslowski, B. B. Stefanov, A. Nanayakkara, M. Challacombe, C. Y. Peng, P. Y. Ayala, W. Chen, M. W. Wong, J. L. Andres, E. S. Replogle, R. Gomperts, R. L. Martin, D. J. Fox, J. S. Binkley, D. J. Defrees, J. Baker, J. P. Stewart, M. Head-Gordon, C. Gonzalez, and J. A. Pople, Gaussian 94, Revision B.1, Gaussian, Inc., Pittsburgh, 1995.
4. T. H. Dunning, Jr., *J. Chem. Phys.* **53**, 2823 (1970).
 5. A. Schafer, H. Horn, and R. Ahlrichs, *J. Chem. Phys.* **97**, 2571 (1992).
 6. T. H. Dunning, Jr., *J. Chem. Phys.* **90**, 1007 (1989).
 7. M. W. Schmidt, K. K. Baldridge, J. A. Boatz, S. T. Elbert, M. S. Gordon, J. H. Jensen, S. Koseki, N. Matsunaga, K. A. Nguyen, S. Su, T. L. Windus, M. Dupuis, and J. A. Montgomery, Jr., *J. Comp. Chem.* **14** 1347 (1993).
 8. J. Oddershede, notes from a series of lectures given at the University of Utah, April 1991.
 9. K. A. Jameson and C. Jameson, *Chem. Phys. Lett.* **134**, 461 (1987).
 10. A. Pines, M. G. Gibby, and J. S. Waugh, *Chem. Phys. Lett.* **15**, 373 (1972).
 11. T. M. Duncan and R. W. Vaughan, *J. Catalysis* **67**, 49 (1981).